

Singlet scalar dark matter in the non-commutative space-time: a viable hypothesis to explain the gamma-ray excess in the galactic center

Zahra Rezaei*

Faculty of Physics, Yazd University, P.O. Box 89195-741, Yazd, Iran

S. Peyman Zakeri†

School of Particles and Accelerators,

Institute for Research in Fundamental Sciences (IPM), P.O.Box 19395-5531, Tehran, Iran

(Dated: July 6, 2020)

Abstract

We explore the non-commutative space-time to revive the idea that gamma-ray excess in the galactic center can be the result of particle dark matter annihilation. In the non-commutative theory, the photon spectrum is produced by direct emission during this annihilation where a photon can be embed in the final state together with other direct products in new vertices. In the various configurations of dark matter phenomenology, we adopt the most common model known as singlet scalar. Calculating the relevant aspects of the model, we can obtain the photon flux in the galactic center. Comparing our numerical achievements with experimental data reveals that non-commutative space-time can be a reliable framework to explain the gamma-ray excess.

PACS numbers: 13.90.+i

*Electronic address: zahra.rezaei@yazd.ac.ir

†Electronic address: peyman.zakeri@ipm.ir

I. INTRODUCTION

Current studies on dark matter (DM) in ultra galaxy scales have opened a new window for high energy physics researches. Identifying this unseen non-baryonic matter in the energy density of the universe has provided fundamental physical insights into particle physics, gravity, and even neutrino physics. As there is no candidate in the standard model (SM) of particle physics to constrain the observed DM, various frameworks in the beyond have applied to introduce viable candidate(s) on the model-building. Weakly interacting massive particles (WIMPs) [1–4] are found to be the most reliable hypothesis in which DM particles are produced by thermal mechanism called freeze-out. In the other well-motivated scenario, feebly interacting massive particles (FIMPs)[5–8] are created non-thermally in a sense through an opposite process to the former case, known as the freeze-in.

Large efforts have been made to detect DM particles through direct and indirect processes. Direct detection experiments, such as XENON [9], LUX [10], SuperCDMS [11], PANDAX-II [12] and ect. attempt to detect the nuclear recoil in the scattering of DM particles off target nuclei. On the other hand, DM particles can undergo self annihilation and the resulting products are strongly pursued for purposes of indirect detection. These products could be the SM particles such as electrons, positrons, protons, antiprotons, photons and neutrinos.

High energy photons are highly considered as the DM signal. Their excess is followed by astronomical instruments and is well measured in the Galactic Center (GC) by the Fermi Large Area Telescope (Fermi-LAT) [13]. GC gamma-ray excess may also arise from millisecond pulsars [14] and cosmic-rays point sources [15] but the predominant paradigm which persuasively explains this excess is the annihilation of DM [16–18] .

DM annihilation as explanation of gamma-ray excess has been dedicated in a lot of works recently [19–22]. In principle, DM candidates may annihilate to the SM particles (usually when they are gravitationally trapped inside high dense regions such as GC or etc.) and then, a hard photon can be described as final-state radiation. Such high energy photons can also arise from the decay of a metastable DM candidate and, like the former scenario, interpreted as secondary particles [23]. It should be noted that study of DM through its annihilation products like photon can reveal also the information about X-ray signal [24–27] (observed from the Andromeda galaxy (M31) and Perseus cluster) which is not favored in this paper.

Different candidates have been suggested as DM particles, such as scalars [28–31], fermions [32–34], vectors [35, 36], ect. [37–39]. The singlet scalar DM model is the simplest one which contains just two free parameters [31]. In this model, DM particles annihilate to the SM particles via the usual Higgs particle. Since photon does not couple with Higgs (and any other neutral particle) straightly, and the final state consists of photon(s) dose(do) not exist in the tree level, all investigated photon excess have been performed in the higher order of perturbation theory, in the SM.

Generally, γ – or X – ray excesses have been observed in the places containing high dencity of (dark) matter, stronge magnetic fields or both of them. In these places, the usual space-time are not reliable. With this motivation in mind, we consider the non-commutative space-time (NCST) framework to explain the gamma-ray excess in the GC.

In the NCST, photon can be coupled with neutral particles. Therefore, photon couples with Higgs [40], in addition to be the direct product of scalar DM decays [41]. In this work, we aim to produce the gamma by prompt processes in which DM particles can directly decay to a photon in the NCST. This consideration results in less vertices and also sufficient photon flux in an accurate way.

The article is organized as follows. In section II, we introduce the construction of the NCST and propose our singlet scalar DM model in this space-time. The GC gamma-ray excess is phenomenologically presented in Sec. III, where we have also described its numerical calculations. Aiming to identify the viable parameter space, we also investigate the cross section of DM annihilation and discuss the final implications and results in Sec. IV. Concluding remarks and also future points of view are summarized in Sec. V.

II. NON-COMMUTATIVE SPACE-TIME (NCST)

In the following, we study the NCST theory and the singlet scalar DM properties in this theory.

A. THE NCST THEORY

A significant and fundamental point in the NCST is the commutation relation between the coordinates in the canonical version, i.e.

$$[\hat{x}^\mu, \hat{x}^\nu] = i\theta^{\mu\nu}, \quad (1)$$

where \hat{x}^μ and \hat{x}^ν read as operators and $\theta^{\mu\nu}$ is a constant, real and anti-symmetric tensor. $\theta^{\mu\nu}$ is the non-commutative (NC) parameter with the length squared dimension (L^2) and is related to the NC energy scale Λ_{NC} as $\Lambda_{NC} \approx (\sqrt{|\theta^{\mu\nu}|})^{-1}$. To pass from ordinary space to NC one, commutative fields and the ordinary product between them should be replaced respectively by NC fields and the star product which can be described as

$$(f * g)(x) = \exp\left(\frac{i}{2}\theta^{\mu\nu} \frac{\partial}{\partial x^\mu} \frac{\partial}{\partial x^\nu}\right) f(x)g(y)|_{y \rightarrow x}, \quad (2)$$

where $f(x)$ and $g(y)$ are regular functions on R^n . Moving to NCST causes some problems such as charge quantization [42] and gauge group definition [43]. There are two approaches to overcome these concerns. The first one is Seiberg-Witten (SW) map whereby the gauge group is the SM gauge group $SU(3) \times SU(2) \times U(1)$ and NC fields are extended in terms of ordinary ones [44]. The second approach makes the gauge group larger into $U_*(3) \times U_*(2) \times U_*(1)$, then using Higgs mechanism reaches to the SM gauge group [45]. Writing field theory in the NCST (via the aforementioned approaches) causes new features which creates new vertices and corrects the ordinary ones in the SM [46–49]. Antisymmetric tensor $\theta^{\mu\nu}$ has six independent components according to $\theta^{\mu\nu} = (\theta^{0i}, \theta^{ij})$ with $i, j = 1, 2, 3$. Since the unitarity of the theory is violated for $\theta^{0i} \neq 0$ [50], the limit $\theta^{0i} = 0$ is chosen. Also, at the leading order we preserve our calculations up to order $\theta^{\mu\nu}$ (defined as $O(\theta)$ hereafter). In this paper, we employ SW map and use the calculated vertices in [40].

B. Singlet Scalar DM in the NCST

One of the most simple and minimal SM extension to describe the particle candidate of DM is made by adding a real singlet scalar particle such that it can reach the equilibrium with the bath particles and plays the role of WIMP DM [31, 51–55]. In the sequent model, DM can interact with the thermal soup through the Higgs portal and its stability is usually

guaranteed by a discrete Z_2 symmetry. The framework of this model is parameterized as:

$$\mathcal{L} = \mathcal{L}_{SM} + \frac{1}{2}\partial_\mu S \partial^\mu S - \frac{m_0^2}{2}S^2 - \frac{\lambda_S}{4}S^4 - \lambda_{HS}S^2 H^\dagger H. \quad (3)$$

In this literature, S denotes the DM and H is the $SU(2)$ Higgs doublet. After spontaneous symmetry breaking, Higgs doublet follows as

$$H = \frac{1}{\sqrt{2}} \begin{pmatrix} 0 \\ v_H + h \end{pmatrix}, \quad (4)$$

where $v_H = 246$ GeV reads as vacuum expectation value of Higgs, and the Higgs-scalar Lagrangian changes to

$$\mathcal{L} = \mathcal{L}_{SM} + \frac{1}{2}\partial_\mu S \partial^\mu S - \frac{1}{2}m_S^2 S^2 - \frac{\lambda_S}{4}S^4 - \lambda_{HS}S^2 h^\dagger h - \lambda_{HS} v_H S^2 h, \quad (5)$$

while DM mass is $m_S = \sqrt{m_0^2 + \lambda_{HS}v_H^2}$ and h is the SM-like Higgs observed at the LHC. DM annihilation to the SM particles are displayed in Fig. 1 for the singlet scalar DM model. Higgs is the only intermediate particle that connect the singlet scalar DM to the SM particles. Therefore, all final states depend on the coupling of Higgs and singlet scalar DM that is determined by λ_{HS} .

As mentioned before, photon could couple to the neutral particles in the NCST and the SM particles of final states could be generated from the mediated photon. The first row processes of Fig. 1 could be possible with mediation of photon in the NCST. The scalar-photon coupling and its results had been investigated for the NCST in Ref. [41]. It has been revealed that cross sections are non-zero just for $\theta^{0i} \neq 0$ [41]. The limit $\theta^{0i} = 0$ is chosen in the current work, then it is not required to add the mediated photon results. Also, by anomalous three gauge boson couplings that is probable in NCST [49, 56], the $\gamma\gamma$ final state with mediation of photon is investigated in [57]. Since both vertices are of $O(\theta)$ (and therefore the cross section is of $O(\theta^4)$) we put it away, too.

In the NCST, the photon emission in the final state of a tree-level channel is possible where Higgs is the mediated particle. In this manner, we have some new vertices such as hhZ , $hf\bar{f}\gamma$ and $hW^+W^-\gamma$. Hence, DM can undergo a pair annihilation as $SS \rightarrow f\bar{f}, ZZ, W^+W^-, hh, hZ, f\bar{f}\gamma, W^+W^-\gamma$, where the existed vertices (in the SM) have obtained some corrections from the NCST.

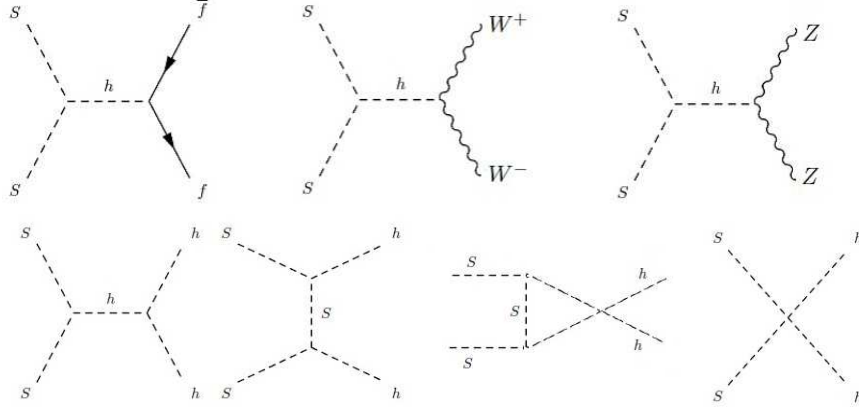


FIG. 1: Tree level diagrams for singlet scalar DM annihilation processes

The SSh and $SShh$ couplings could require some corrections in the NCST. To carry out these vertices, one needs to use the Higgs-scalar action after symmetry breaking

$$\mathcal{L}_{HS} = \int d^4x (\lambda_{HS} \hat{S} * \hat{S} * \hat{h}^\dagger * \hat{h} + \lambda_{HS} v_H \hat{S} * \hat{S} * \hat{h}), \quad (6)$$

where the commutative fields (S and h) and the ordinary product between them are replaced respectively by the non-commutative fields (\hat{S} and \hat{h}) and the star product ($*$). The SW map of the scalar field ($\hat{\phi}$) can be written as

$$\hat{\phi} = \phi + \frac{1}{2} \theta^{\alpha\beta} V_\beta (\partial_\alpha - \frac{i}{2} (V_\alpha \phi - \phi V'_\alpha)) + \frac{1}{2} \theta^{\alpha\beta} (\partial_\alpha - \frac{i}{2} (V_\alpha \phi - \phi V'_\alpha)) V'_\beta + O(\theta^2), \quad (7)$$

where the scalar field (ϕ) transforms via two different gauge groups with their corresponding gauge fields (V and V'). It is straightforward to show that the first order of SSh and $SShh$ couplings in the NCST are of $O(\theta^2)$ and these couplings are removable in the current calculations (It had been shown for hZZ coupling in the NCST [40], too and we put it away).

Extending the NCST with the singlet scalar S embeds three independent parameters as

$$m_S, \lambda_{HS}, \Lambda_{NC}, \quad (8)$$

whereby we probe the model parameter space. In the next section, the calculations of gamma-ray excess are presented.

III. GAMMA-RAY EXCESS

Our main endeavour in this section is to declare the NCST as a new promising framework to explain the excess of gamma-ray in the energy range 1-3 GeV in the region of GC. A powerful study by Calore, Cholis and Weniger (CCW) [58] reveals that this GC extended source can be interpreted as DM annihilation. In this regard, latter works have found that such an excess is well fitted with DM interpretation where an annihilation cross section times velocity $\langle\sigma v\rangle \propto 10^{-27} - 10^{-26} \text{cm}^3/\text{s}$ [18, 59–62] is required. In the following, we will investigate whether a WIMP like singlet scalar DM can generate sufficient GC gamma-ray flux in the NCST. The spectrum and amplitude of the gamma-ray signal will be considered for processes in which DM particles annihilate to the SM final states through s -channel.

The differential (prompt) photon flux resulting from annihilation of DM particles is given by [63]

$$\frac{d^2\Phi}{d\Omega dE} = \left(\frac{r_\odot}{8\pi}\right) \left(\frac{\rho_\odot}{m_S}\right)^2 J \cdot \sum_f \langle\sigma v\rangle_{i\rightarrow f} \frac{dN_\gamma^f}{dE}, \quad (9)$$

where r_\odot is the distance between the Sun and the GC, i.e. 8.33 kpc and ρ_\odot is the DM density at the solar location with the canonical value $\approx 0.3 \text{ GeV}/\text{cm}^3$ [64]. The J factor encodes the effect of matter in line of sight and is given by:

$$J = \int_{\text{l.o.s}} \frac{dr'}{r_\odot} \left(\frac{\rho(r(r', \theta))}{\rho_\odot} \right)^2, \quad (10)$$

where r_\odot and ρ_\odot are added by convention to make J dimensionless. Also, note that $\langle\sigma v\rangle_{i\rightarrow f}$ is the cross section of DM (i) annihilation to the final states (f) and dN_γ^f/dE is the energy spectrum of photons produced per one annihilation specifically for the aforementioned final state. The relevant calculations for annihilation cross section are presented in the Appendix. For the integrated flux over a region $\Delta\Omega$, we need to average the J factor over that region:

$$\bar{J}(\Delta\Omega) = \frac{\int_{\Delta\Omega} J d\Omega}{\Delta\Omega}, \quad (11)$$

for example if we are interested in $10^\circ \times 10^\circ$ region around the GC, $\Delta\Omega = 0.121$ steradians and $\bar{J} = 77.7$ [63], if we assume the Navarro-Frenk-While (NFW) profile for DM [65, 66].

As mentioned in Ref. [63], the DM halo profiles are the same for local environment (few pc away from the Earth), but for distances closer to the GC they diverge. Therefore, the

calculations for GC region can be sensitive to the choice of the DM profile. According to this gamma emission picking at GC, we assume spherically symmetric and centrally peaked DM halo profile follows NFW as bellow

$$\rho(r) = \rho_s \frac{(r/r_s)^{-\gamma}}{(1 + r/r_s)^{3-\gamma}}, \quad (12)$$

with the typical scale density $\rho_s = 0.4 \text{ GeV/cm}^3$, the radius scale $r_s = 20 \text{ kpc}$ and a varied inner slop parameter γ . In order to calculate the differential flux toward Galactic coordinates, we follow the same choices of parameters as in Ref. [67], i.e. our region of interest (ROI) is at Galactic longitude $|l| \leq 20^\circ$ and Galactic latitude $2^\circ \leq |b| \leq 20^\circ$ where the inner slop parameter is adopted as $\gamma = 1.2$ and energy bins (Eq. (2.2) in Ref [67]) read as $n_{\text{bins}} = 20$ in the range $[500\text{MeV}, 500\text{GeV}]$.

The averaged J -factor for this ROI is also given by: $\bar{J} = 49.13$. We now calculate the energy spectrum of photons denoted as dN_γ/dE . Before spectral exploration, a discussion is in order. As it was mentioned earlier in Sec. I, we aim to produce prompt photon flux in the leading order of DM annihilation. Thus we consider processes in which photon is produced directly by DM pair annihilation. In this manner, DM particles can annihilate into pure $\bar{b}b\gamma$, $\bar{t}t\gamma$, $\tau^+\tau^-\gamma$ and $W^+W^-\gamma$ channels accompanied with also combinations of them.

To do this, first we start with PPPC4DMID package [63] as a particle physicist cookbook on calculation of DM signals. Although, PPPC4DMID is a usual instrument to generate photon excess in the SM, the only processes that are considered are DM DM \rightarrow primary primary, where "primary" is a particle of the SM, and photons are produced in the loop levels by the electroweak gauge bosons. Thus, we can not use this package in our presented setup of producing gamma-ray.

In this regard, due to the uncertainty of the GC gamma-ray source, we can perform general log-parabola analysis for the spectrum as [20, 68]

$$\frac{dN_\gamma}{dE} = N_0 \left(\frac{E}{E_b} \right)^{-(\alpha + \beta \log(E/E_b))}, \quad (13)$$

where α and β are halo parameters and E_b is an arbitrary energy scale. N_0 is the number of photons per square centimetre per second per steradian and denotes the possibility of photon emitted per annihilation event. As we produce photon promptly per annihilation channel through its coupling with the Higgs in the NCST, thus, neglecting higher orders of perturbation, we set $N_0 = 1$ in our formalism.

Now, the value of α and β parameters ought to be determined. PYTHIA 6.4 [69] is usually used to simulate SM processes that gives rise to the spectrum of photons (as well as other particle spectra). In this case, gamma can be described as final-state radiation of charged particles (e.g. bremsstrahlung spectrum) or neutral ones (e.g. decays of π^0). In the case of DM interpretation, the aforementioned particles also generate from DM annihilation or decay [19]. As our model (singlet scalar DM in the NCST) involves new elementary couplings that generates a different kind of photon flux, we can not utilize PYTHIA and need to calculate the matrix element for photon emission manually. We will do this in Sec. IV and investigate the best fit of our model in terms of the halo parameters and contributing channels.

Regarding the energy spectrum of photons, it should be noted here that we can employ various spectral models (e.g. one with exponential cutoff [20]) but we have found the logarithmic form (Eq. 13) with the best consistency. On the other hand, we should emphasize that dN_γ/dE is a property of the annihilation process and does not depend on the halo density profile. Hence, one may also choose Einasto [70, 71] or $\alpha\beta\gamma$ profiles [20, 68].

In the following, we investigate the model parameter space with DM annihilation cross section and the generation of gamma-ray excess is inquired.

IV. RESULTS AND DISCUSSION

The viability of the procedure introduced in previous sections is tested over a range of model parameters space in this section.

Referring to [72], we divide DM mass range into several intervals. The adopted mass range of DM determines the relevant processes through which DM can be annihilated. Our results are best behaved in three intervals. The first interval is around the weak gauge bosons masses (80 – 100 GeV), the second one is selected around Higgs mass (120 – 170 GeV which is smaller than the top quark mass) and the third region is bigger than the top quark mass (> 173 GeV). In all calculations, the light fermions (e, μ, ν_i, u, d, s and c) are ignored.

We explore the parameter space consistent with the phenomenological predictions of thermal averaged cross section times velocity of DM annihilation, $\langle \sigma v \rangle$, and differential photon flux from DM annihilations, $E^2 d\Phi/dE$. To find the correlation between variables

λ_{HS} , m_S and Λ_{NC} , the scatter points (λ_{HS}, m_S) and (Λ_{NC}, m_S) are investigated.

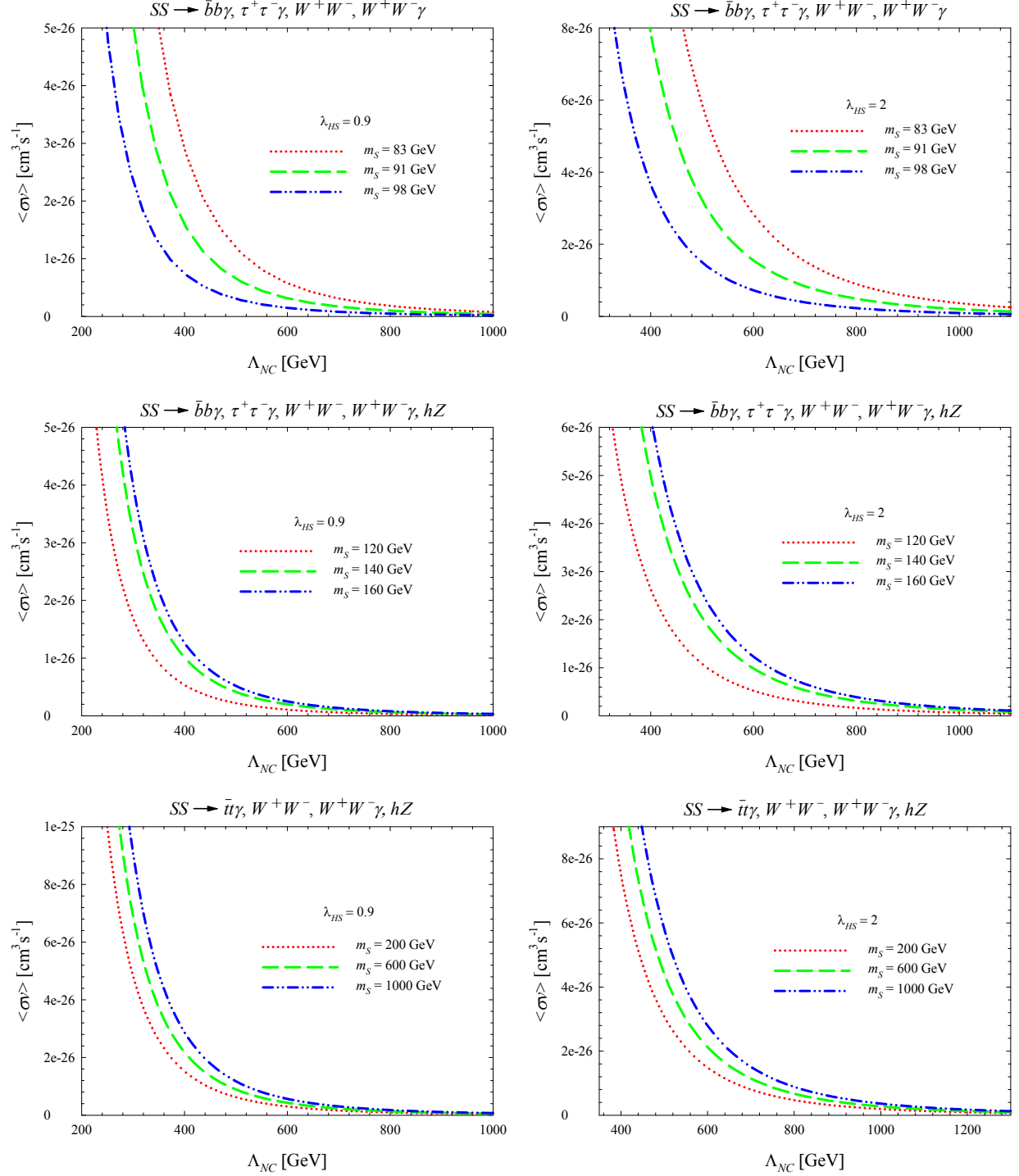


FIG. 2: DM annihilation cross section in terms of NC energy scale. In this figure, all contributing channels are considered. For different values of m_S , we set $\lambda_{HS} = 0.9$ (left panel) and $\lambda_{HS} = 2$ (right panel).

Figure 2 describes $\langle \sigma v \rangle$ versus Λ_{NC} . It shows that $\langle \sigma v \rangle$ decreases for all DM mass intervals. The final states of DM annihilation are chosen as shown in the above of each plot of Fig. 2, according to the relevant DM mass. In the first region, the DM annihilation reads as $SS \rightarrow f\bar{f}, f\bar{f}\gamma, ZZ, W^+W^-, W^+W^-\gamma$ where fermion f indicates τ lepton and b quark. In pure NCST, $SS \rightarrow f\bar{f}$ is zero and $SS \rightarrow ZZ$ is of order ($> \theta^2$), therefore they don't play any role in our considerations. In the second region, DM particles undergo an annihilation through $SS \rightarrow f\bar{f}, f\bar{f}\gamma, ZZ, W^+W^-, W^+W^-\gamma, Zh, hh$ where only the final states $f\bar{f}\gamma, W^+W^-, W^+W^-\gamma, Zh$ (which f is still to be defined as τ and b particles) are adopted in NC hypothesis. The threshold energy to produce Zh is around 108 GeV, therefore we have chosen the DM mass range few GeVs bigger and so nearer the Higgs mass. The third analysis devotes to the heavy massive DM where its mass varies from 173 GeV to 1 TeV. The contributing processes for DM annihilation are the same as former cases except that f indicates top quark here. As shown in Fig. 2, increasing DM mass or/and Higgs-DM coupling (λ_{HS}), the desired cross section acquires in the larger Λ_{NC} .

The DM annihilation cross section $\langle \sigma v \rangle$ with respect to λ_{HS} is depicted in Fig. 3. Three DM mass regions are defined again. Left plots are depicted for the fixed Λ_{NC} and three different masses in each region and the fixed mass with different Λ_{NC} s are shown in the right side. As it shows, the cross section increases in terms of λ_{HS} .

Figure 4 describes $\langle \sigma v \rangle$ versus m_S for three regions of DM mass. For lighter DM particles (in the first region), $\langle \sigma v \rangle$ decreases with respect to the mass but for the heavier ones, where the new hhZ coupling is appeared from the NCST effects, the slow increment in cross section behaviour is seen.

We have performed our calculations with DM mass as it could generate the Higgs particle (around $m_S \cong 62.5\text{GeV}$), but we didn't obtain desired cross section. As the observed relic density of DM is the most important aspect of DM phenomenology, we consider (λ_{HS}, m_S) -plane in such a way that it could satisfy the experimental measurements [72]. The new (Λ_{NC}, m_S) -plane is also considered to investigate the NCST effect on the parameter space. The scatter points in the (λ_{HS}, m_S) -plane and (Λ_{NC}, m_S) -plane are depicted in Figs. 5 and 6, respectively. In Fig. 5, the process is incremented for the first range of mass and is decremented for two others, for a fixed Λ_{NC} . (Λ_{NC}, m_S) -plane is depicted for two different values of λ_{HS} (see Fig. 6). The processes are the same for both λ_{HS} , but the difference goes back to the Λ_{NC} amounts; the bigger amount of λ_{HS} is, the larger amount of Λ_{NC} it is.

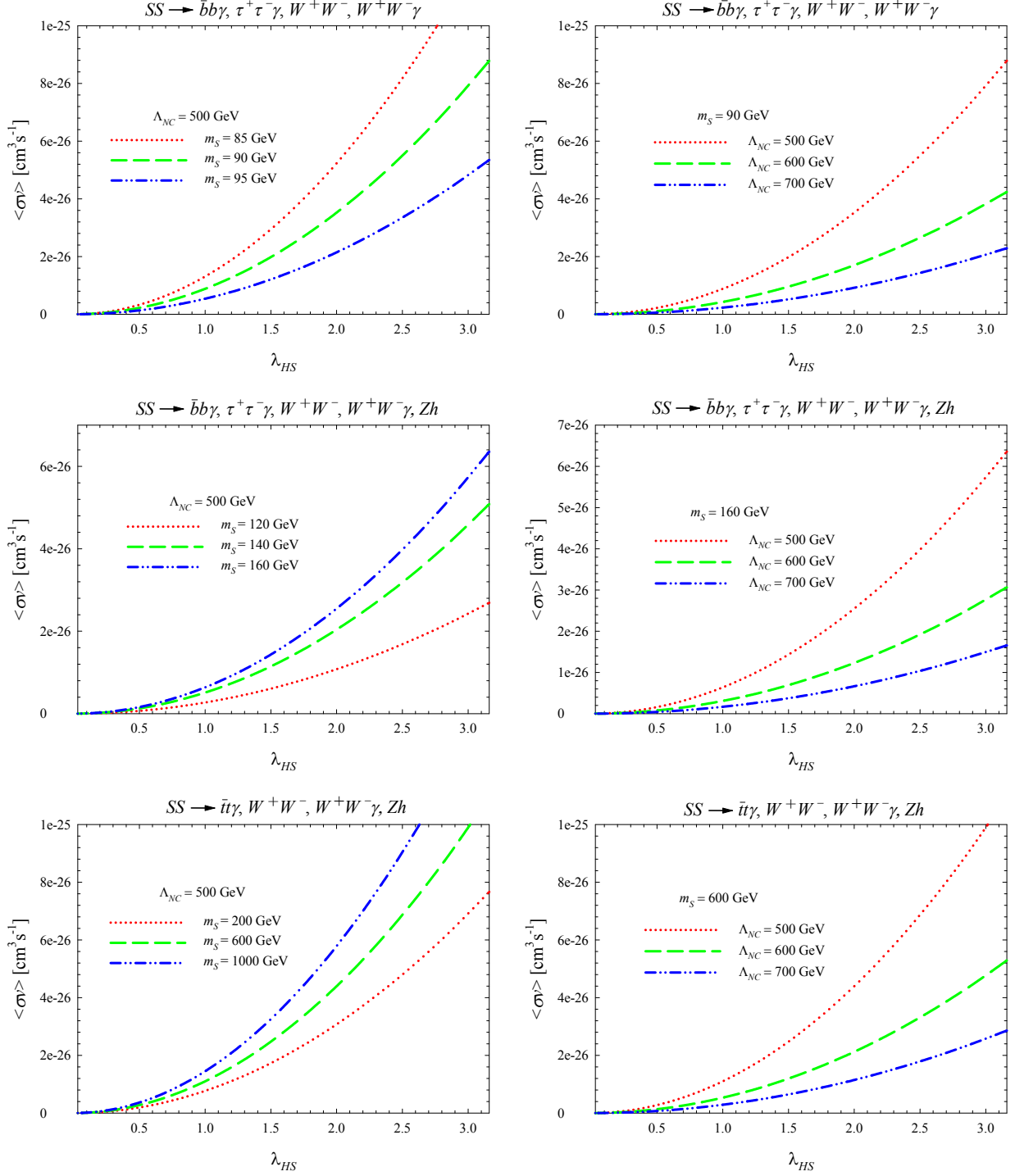


FIG. 3: DM annihilation cross section in terms of its coupling. In this figure, all contributing channels are considered. In the left panel, we set $\Lambda_{NC} = 500$ GeV for different values of m_S and in the right one corresponding values of m_S are adopted for different choices of Λ_{NC} .

Explaining the gamma excess within the framework of singlet scalar DM is our main

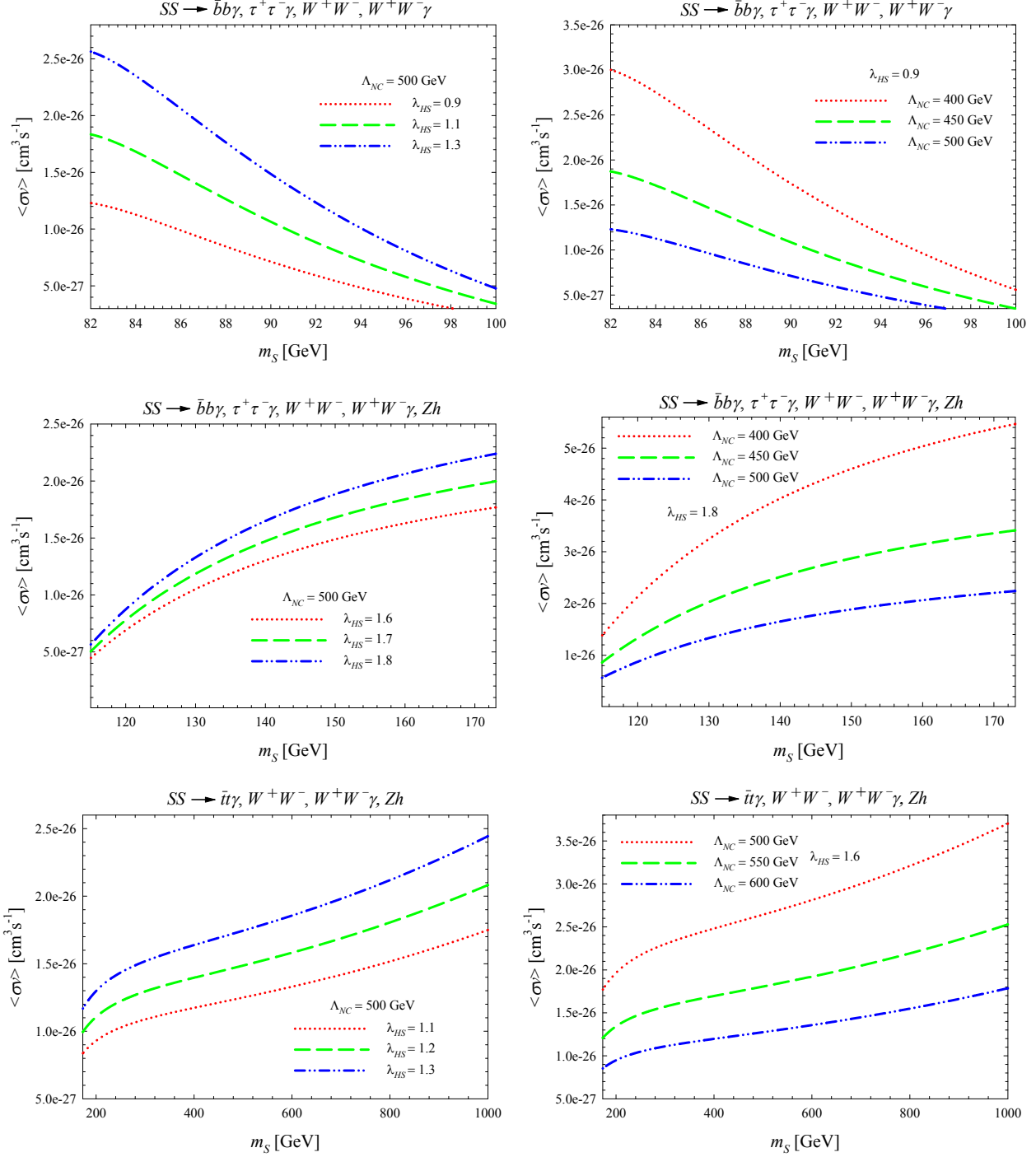


FIG. 4: DM annihilation cross section in terms of its mass. In this figure, all contributing channels are considered. In the left panel, we set $\Lambda_{NC} = 500$ GeV for different values of λ_{HS} and in the right one corresponding values of λ_{HS} are adopted for different choices of Λ_{NC} .

purpose in the presenting paper. Thus we analyze Fermi-LAT data via evaluating the

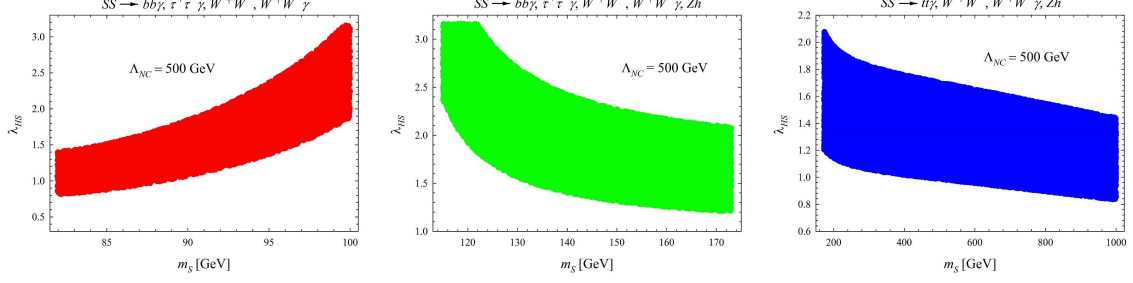


FIG. 5: The allowed region in the (λ_{HS}, m_S) -parameter space where $\Lambda_{NC} = 500$ GeV. The panels are labeled by their corresponding channels.

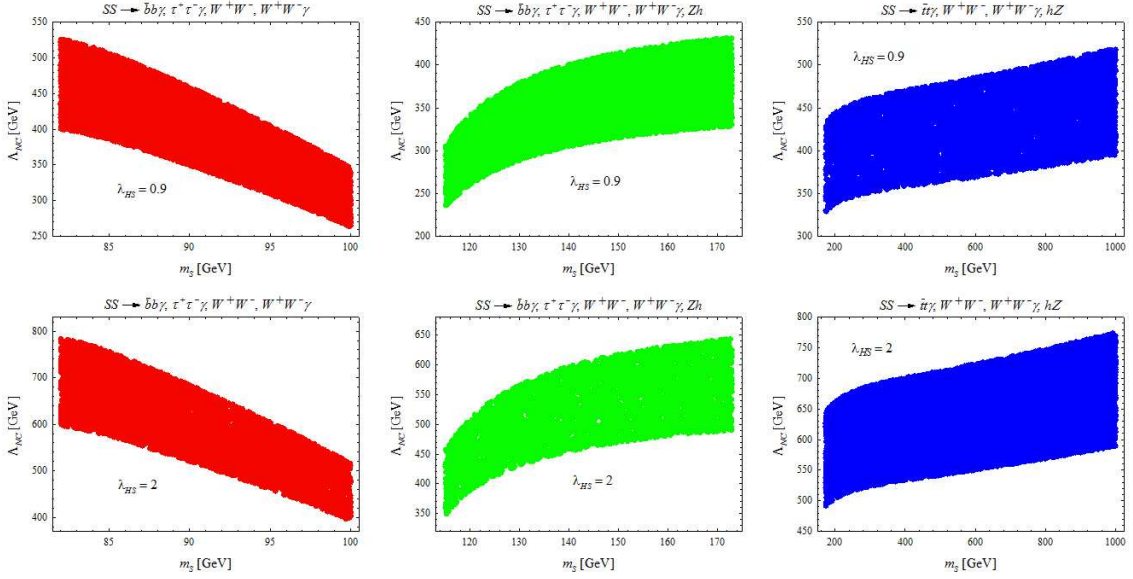


FIG. 6: The allowed region in the (Λ_{NC}, m_S) -parameter space where two different values are adopted for λ_{HS} . The panels are labeled by their corresponding channels.

gamma-ray flux in our model. As we mentioned earlier in Sec. III, we adopt $\alpha\beta\gamma$ approach and NFW halo profile for DM using the appropriate Galactic parameters ($|l| \leq 20^\circ$, $2^\circ \leq |b| \leq 20^\circ$). The photon flux for different benchmark points (BPs) is shown in Fig. 7. Benchmark sets are tabulated in tables I–III where we have found the best fit model in the gamma-ray energy range of 1 – 3 GeV. Considering the $SS \rightarrow W^+W^-\gamma$ channel at $\Lambda_{NC} = 500$ GeV (upper panel in Fig. 7), our best fit values include DM mass as $m_S = 100, 300, 500$ GeV and its coupling as $\lambda_{HS} = 0.9, 1.6, 2$. The upper panel of Fig. 7 shows the comparison of model flux with Fermi-LAT data using BP1, BP2 and BP3, where the best fit spectra are for fixed energy $E_b = 100$ GeV accompanied with relevant α, β values given in Table I.

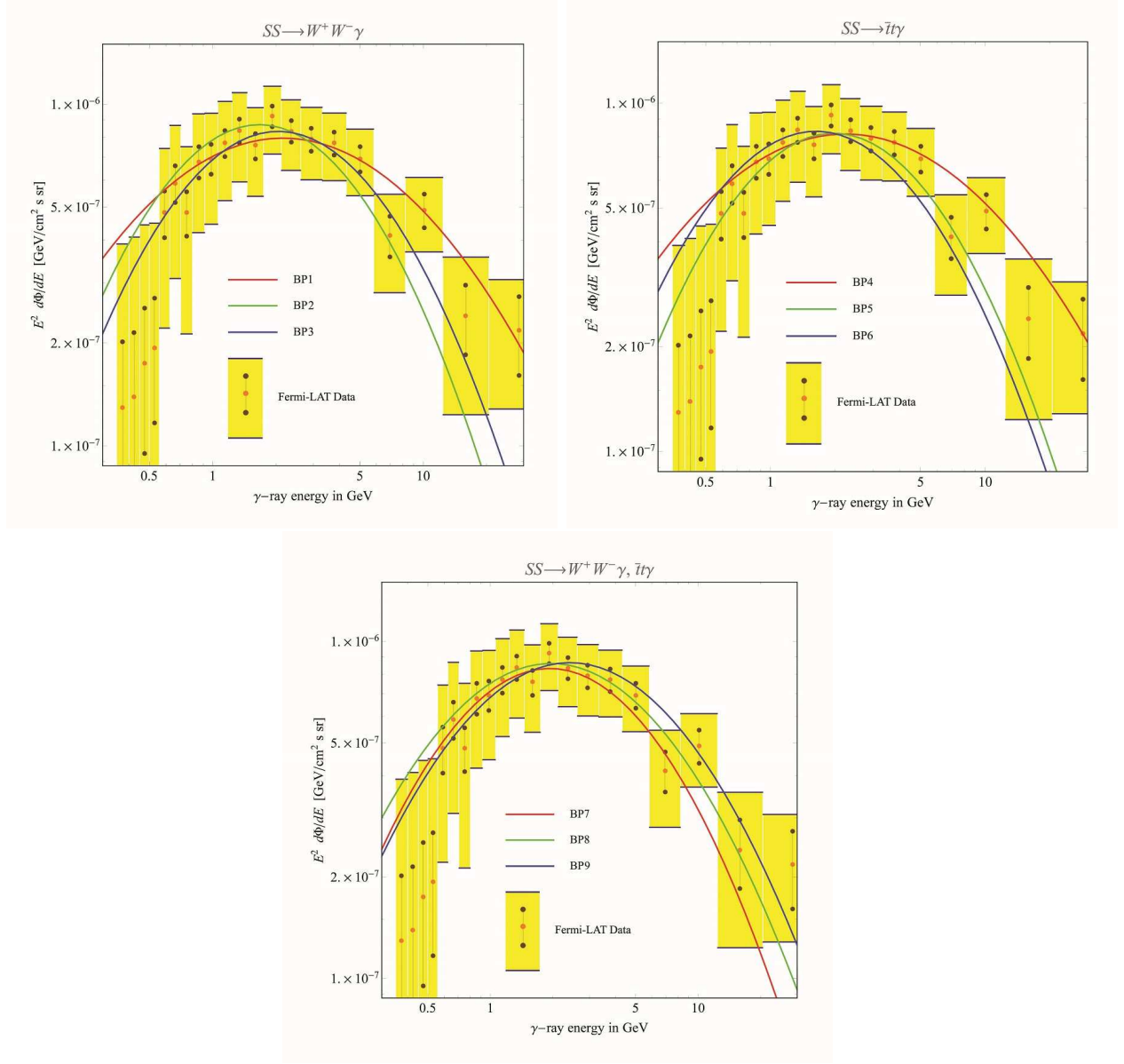


FIG. 7: Gamma-ray flux obtained from singlet scalar annihilation in the NCST in comparison with Fermi-LAT results. Allowed sets of parameters are presented in the form of nine BPs.

Our next analysis devotes to the DM annihilation into $t\bar{t}\gamma$ and the NC energy scale is chosen as $\Lambda_{NC} = 500$ GeV. The best fit model is again categorized into three BPs (BP4, BP5 and BP6) including different DM masses and couplings where they are chosen as $m_S = 200, 500, 1000$ GeV and $\lambda_{HS} = 3$ depicted in the middle panel of Fig. 7. Appropriate α, β are presented in Table II where the best consistency of our model is at $E_b = 300$ GeV.

Considering two aforementioned contributions in DM annihilation, now we investigate

$SS \rightarrow W^+W^-\gamma, \bar{t}t\gamma$ channels to explore the model flux (lower panel of Fig. 7). Comparing with Fermi-LAT data, we reach to the model best fit given in Table III. In BP7, BP8 and BP9 sets, m_s ranges as 500, 700, 1000 GeV and λ_{HS} reads as 0.9, 1.6, 2 respectively, for $\Lambda_{NC} = 500$ GeV. Log-parabola spectrum indicates the parameters α, β with appropriate values at fixed energy $E_b = 150$ GeV.

In all above analyses, it is obvious from Figs. 7 that the best consistency occurs at the energy range of 1-3 GeV for gamma-ray emission in a centrally peaked form same as the reported map of the excess spectrum in the GC. It should be noted here that $SS \rightarrow \bar{b}b\gamma, \tau^+\tau^-\gamma$ channels are allowed but their contributions are small relative to the aforementioned ones (because of the small mass of b quark and τ lepton against the W boson and t quark).

TABLE I: Bench mark points for $SS \rightarrow W^+W^-\gamma$

BP	α	β	E_b GeV	m_s GeV	λ_{HS}	Λ_{NC} GeV
1	2.6	0.48	100	100	0.9	500
2	4.1	0.9	100	300	1.6	500
3	3.87	0.85	100	500	2	500

TABLE II: Bench mark points for $SS \rightarrow \bar{t}t\gamma$

BP	α	β	E_b GeV	m_s GeV	λ_{HS}	Λ_{NC} GeV
4	2	0.24	300	200	3	500
5	4.115	0.74	300	500	3	500
6	4.69	0.85	300	1000	3	500

V. CONCLUSION

Fermi-LAT probes have opened a new window to pursue DM traces in the GC. Among a lot of theories suggesting the DM interpretation for this cosmic anomaly, we have evaluated singlet scalar particles as WIPM candidates for DM in the framework of the NCST. Extending the NCST beyond the SM, we could define new vertices which generate photon

TABLE III: Bench mark points for $SS \rightarrow W^+W^-\gamma, \bar{t}t\gamma$

BP	α	β	E_b GeV	m_s GeV	λ_{HS}	Λ_{NC} GeV
7	4.1	0.82	150	500	0.9	500
8	3.6	0.69	150	700	1.6	500
9	3.513	0.7	150	1000	2	500

directly in the tree level of the SM channels. We have used this paradigm in order to investigate indirect signals of DM and have derived phenomenological constraints on singlet scalar DM features. First, we have calculated annihilation cross section and have depicted its behavior versus model independent parameters. In a complementary analysis, we have searched for allowed region constructed by specific model parameter space. Then we adopted a conservative approach to examine the photon flux reported by Fermi gamma-ray space telescope.

We considered all possible channels for DM annihilation in order to satisfy observational constraints. Dealing with DM-SM sector coupling at $\Lambda_{NC} = 500$ GeV, for masses bellow 100 GeV, λ_{HS} varies from 0.9 to 3 with an increment dependence. In the region $120 \leq m_S \leq 173$ GeV, λ_{HS} decreases from maximum value 3 to 1.2 as a lower bound. For massive DM ($173 \leq m_S \leq 1000$ GeV), we found a lower bound in DM coupling as 0.8 and the upper one to be 2.08 (see Fig. 5). In the (Λ_{NC}, m_S) -plane, we found fits to the NC energy scale depending on DM mass. For low masses, $m_S \leq 100$ GeV, Λ_{NC} reaches up to 800 GeV for interaction strength of $\lambda_{HS} = 2$. Keeping up this λ_{HS} , the upper bound of NC scale changes to $\Lambda_{NC} = 650$ GeV for $120 \leq m_S \leq 173$ GeV and $\Lambda_{NC} = 780$ GeV for $173 \leq m_S \leq 1000$ GeV (see Fig. 6).

In the last analysis, we tested the viability of our model to explain the photon spectrum. For DM annihilation into $W^+W^-\gamma$, we have found three BPs in which the SM particles of mass 100, 300, 500 GeV can generate sufficient gamma-ray flux. In the other pure channel, DM particles annihilate directly to photon via $SS \rightarrow \bar{t}t\gamma$ with DM masses as 200, 500, 1000 GeV. Then a mixture of both channels ($SS \rightarrow W^+W^-\gamma, \bar{t}t\gamma$) was tested and the best fit values were for $m_S = 500, 700, 1000$ GeV requiring coupling $\lambda_{HS} = 0.9, 1.6, 2$ respectively.

Evaluating our results reveals that the NCST could be considered as a promising frame-

work to increase DM annihilation cross section and validate indirect signals of DM detection. Although in this paper, we have investigated gamma-ray excess in the GC, the NCST can be considered as open research subjects in future DM phenomenological studies. Our upcoming works will devote to the other phenomenological aspects of DM in the NCST (including other DM candidate fields such as fermion, vector etc.).

ACKNOWLEDGMENTS

We would like to thank Mohammad Mehdi Eftefaghi for reviewing the manuscript and we are particularly grateful to Manoj Kaplinghat, Can Kilic, Torbjorn Sjostrand, Marco Cirelli and Mohammadreza Zakeri for useful discussions.

APPENDIX

Here, we summarize DM annihilation cross sections presented in our calculations. We can write $\langle\sigma v\rangle_{i\rightarrow f}$ for the annihilation of DM of mass m_S as

$$\langle\sigma v\rangle_{i\rightarrow f} = \frac{1}{16m_S^4 T K_2^2(\frac{m_S}{T})} \int_{4m_S^2}^{\infty} s \sqrt{s - 4m_S^2} K_1(\frac{\sqrt{s}}{T}) (\sigma v)_{i\rightarrow f} ds, \quad (14)$$

where $K_i (i = 1, 2)$ is the modified Bessel function and T denotes the freeze-out temperature. As we have introduced new vertices in our hypothesis, using Eq. 14 may be severe and time consuming. Thus, we use the following expansion (for non-relativistic particles up to the second order) [41]

$$\langle\sigma v\rangle_{i\rightarrow f} \simeq a^{(0)} + \frac{3}{2}a^{(1)}x^{-1} + \frac{15}{8}a^{(2)}x^{-2}, \quad (15)$$

where

$$a^{(n)} = \frac{d^n}{(d\epsilon)^n} \langle\sigma v\rangle_{i\rightarrow f}|_{\epsilon=0}, \quad \epsilon = \frac{s - 4m_S^2}{4m_S^2}, \quad x^{-1} \equiv \frac{T}{m_S}. \quad (16)$$

Following the above equations, we deduce that $a^{(0)} = a^{(1)} = 0$ and for $a^{(2)}$ we have

$$a^{(2)} = \frac{2x}{K_2^2(x)} \left(\frac{d}{d\epsilon} [\sqrt{\epsilon}(\epsilon + 1) K_1(2x\sqrt{\epsilon + 1})] (\sigma v)_{i\rightarrow f} \right) \Big|_{\epsilon=0}. \quad (17)$$

Substituting $a^{(0)}, a^{(1)}, a^{(2)}$ in Eq. 15, we obtain the following form for DM annihilation cross section

$$\langle\sigma v\rangle_{i\rightarrow f} = \frac{15}{4x K_2^2(x)} \left(\frac{d}{d\epsilon} [\sqrt{\epsilon}(\epsilon + 1) K_1(x)(2x\sqrt{\epsilon + 1})] (\sigma v)_{i\rightarrow f} \right) \Big|_{\epsilon=0}. \quad (18)$$

All the contributing cross sections presented in $(\sigma v)_{i \rightarrow f}$ follow as

$$(\sigma v)_{i \rightarrow f} = (\sigma v)_{SS \rightarrow W^+ W^-} + (\sigma v)_{SS \rightarrow h Z} + (\sigma v)_{SS \rightarrow f \bar{f} \gamma} + (\sigma v)_{SS \rightarrow W^+ W^- \gamma}, \quad (19)$$

and they are expressed as bellow

$$(\sigma v)_{SS \rightarrow W^+ W^-} = \frac{\lambda_{HS}^2 m_W^4}{8\pi} \frac{\sqrt{s - 4m_W^2}/(s\sqrt{s})}{(s - m_h^2)^2 + m_h^2 \Gamma_h^2} \Lambda_{NC}^{-4} (s + m_h^2)^2 \left(\frac{s}{4m_W^2} - 2 \right), \quad (20)$$

$$(\sigma v)_{SS \rightarrow h Z} = \frac{\lambda_{HS}^2 m_Z^2}{8\pi} \frac{(s - m_h^2)^2/(s\sqrt{s})}{(s - m_h^2)^2 + m_h^2 \Gamma_h^2} \Lambda_{NC}^{-4} \left(\frac{(s - m_Z^2 + m_h^2)^2}{4s} - m_h^2 \right)^{3/2}, \quad (21)$$

$$\begin{aligned} (\sigma v)_{SS \rightarrow f \bar{f} \gamma} &= \int_0^1 \int_0^1 \int_0^1 \int_0^1 \int_1^{\frac{s-4m_f^2}{2\sqrt{s}}} \frac{|\mathcal{M}_{SS \rightarrow f \bar{f} \gamma}|^2}{F} \\ &\times \frac{1}{(4\pi)^3} \sqrt{1 - \frac{4m_f^2}{s - 2\sqrt{s}E}} 2E dE dx_2 dx_3 dx_4 dx_5, \end{aligned} \quad (22)$$

$$\begin{aligned} (\sigma v)_{SS \rightarrow W^+ W^- \gamma} &= \int_0^1 \int_0^1 \int_0^1 \int_0^1 \int_1^{\frac{s-4m_W^2}{2\sqrt{s}}} \frac{|\mathcal{M}_{SS \rightarrow W^+ W^- \gamma}|^2}{F} \\ &\times \frac{1}{(4\pi)^3} \sqrt{1 - \frac{4m_W^2}{s - 2\sqrt{s}E}} 2E dE dx_2 dx_3 dx_4 dx_5, \end{aligned} \quad (23)$$

where $F = \sqrt{s(s - 4m_S^2)}$ and the relevant amplitudes are given by

$$|\mathcal{M}_{SS \rightarrow f \bar{f} \gamma}|^2 = \frac{4\lambda_{HS}^2 e^2 Q_f^2 m_f^2}{(s - m_h^2)^2 + m_h^2 \Gamma_h^2} \frac{E^2 (E_f^2 - m_f^2)}{\Lambda_{NC}^4} (\sqrt{1 - x_2^2}) (\sqrt{1 - x_4^2}), \quad (24)$$

$$\begin{aligned} |\mathcal{M}_{SS \rightarrow W^+ W^- \gamma}|^2 &= \frac{8\lambda_{HS}^2 e^2 m_W^4}{(s - m_h^2)^2 + m_h^2 \Gamma_h^2} \frac{E^2}{\Lambda_{NC}^4} \left\{ \frac{4}{3} - \frac{2}{3m_W^4} \right. \\ &\times \left[(2E_W^2 - m_W^2 - E^2 + EE_W)^2 + 2E(E_W - \frac{E}{2})(2E_W^2 - m_W^2 - \frac{E^2}{2}) \right. \\ &+ \frac{3}{2}(E_W^2 - m_W^2)(2E_W^2 + \frac{E^2}{2} - 2EE_W) \sqrt{(1 - x_2^2)(1 - x_4^2)} \\ &\left. \left. - \frac{8}{3m_W^2} \left[(2EE_W - E^2 - m_W^2) + \frac{3}{4}(E_W^2 - m_W^2) \sqrt{(1 - x_2^2)(1 - x_4^2)} \right] \right] \right\}. \end{aligned} \quad (25)$$

Here, e and Q_f are the electric charge of electron and of fermion f respectively. Energies E_f and E_W are also defined in terms of gamma-ray energy E as

$$E_{f/W} = \frac{\sqrt{s} - E}{2}. \quad (26)$$

-
- [1] P. Gondolo and G. Gelmini, Nucl. Phys. B **360** (1991), 145-179 doi:10.1016/0550-3213(91)90438-4
 - [2] M. Srednicki, R. Watkins and K. A. Olive, Nucl. Phys. B **310** (1988), 693 doi:10.1016/0550-3213(88)90099-5
 - [3] H. Y. Chiu, Phys. Rev. Lett. **17** (1966), 712 doi:10.1103/PhysRevLett.17.712
 - [4] S. Yaser Ayazi, A. Mohamadnejad and S. P. Zakeri, Mod. Phys. Lett. A **33** (2018) no.27, 1850159 doi:10.1142/S0217732318501596 [arXiv:1804.02876 [hep-ph]].
 - [5] J. McDonald, Phys. Rev. Lett. **88** (2002), 091304 doi:10.1103/PhysRevLett.88.091304 [arXiv:hep-ph/0106249 [hep-ph]].
 - [6] L. J. Hall, K. Jedamzik, J. March-Russell and S. M. West, JHEP **03** (2010), 080 doi:10.1007/JHEP03(2010)080 [arXiv:0911.1120 [hep-ph]].
 - [7] S. Yaser Ayazi, S. M. Firouzabadi and S. P. Zakeri, J. Phys. G **43** (2016) no.9, 095006 doi:10.1088/0954-3899/43/9/095006 [arXiv:1511.07736 [hep-ph]].
 - [8] S. Peyman Zakeri, S. Mohammad Moosavi Nejad, M. Zakeri and S. Yaser Ayazi, Chin. Phys. C **42** (2018) no.7, 073101 doi:10.1088/1674-1137/42/7/073101 [arXiv:1801.09115 [hep-ph]].
 - [9] E. Aprile *et al.* [XENON], Phys. Rev. Lett. **121** (2018) no.11, 111302 doi:10.1103/PhysRevLett.121.111302 [arXiv:1805.12562 [astro-ph.CO]].
 - [10] D. S. Akerib *et al.* [LUX], Phys. Rev. Lett. **118** (2017) no.2, 021303 doi:10.1103/PhysRevLett.118.021303 [arXiv:1608.07648 [astro-ph.CO]].
 - [11] R. Agnese *et al.* [SuperCDMS], Phys. Rev. Lett. **116** (2016) no.7, 071301 doi:10.1103/PhysRevLett.116.071301 [arXiv:1509.02448 [astro-ph.CO]].
 - [12] X. Cui *et al.* [PandaX-II], Phys. Rev. Lett. **119** (2017) no.18, 181302 doi:10.1103/PhysRevLett.119.181302 [arXiv:1708.06917 [astro-ph.CO]].
 - [13] W. B. Atwood *et al.* [Fermi-LAT], Astrophys. J. **697** (2009), 1071-1102 doi:10.1088/0004-637X/697/2/1071 [arXiv:0902.1089 [astro-ph.IM]].

- [14] R. Bartels, S. Krishnamurthy and C. Weniger, Phys. Rev. Lett. **116** (2016) no.5, 051102 doi:10.1103/PhysRevLett.116.051102 [arXiv:1506.05104 [astro-ph.HE]].
- [15] S. K. Lee, M. Lisanti, B. R. Safdi, T. R. Slatyer and W. Xue, Phys. Rev. Lett. **116** (2016) no.5, 051103 doi:10.1103/PhysRevLett.116.051103 [arXiv:1506.05124 [astro-ph.HE]].
- [16] L. Bergstrom, P. Ullio and J. H. Buckley, Astropart. Phys. **9** (1998), 137-162 doi:10.1016/S0927-6505(98)00015-2 [arXiv:astro-ph/9712318 [astro-ph]].
- [17] S. Ipek, D. McKeen and A. E. Nelson, Phys. Rev. D **90** (2014) no.5, 055021 doi:10.1103/PhysRevD.90.055021 [arXiv:1404.3716 [hep-ph]].
- [18] T. Daylan, D. P. Finkbeiner, D. Hooper, T. Linden, S. K. N. Portillo, N. L. Rodd and T. R. Slatyer, Phys. Dark Univ. **12** (2016), 1-23 doi:10.1016/j.dark.2015.12.005 [arXiv:1402.6703 [astro-ph.HE]].
- [19] K. N. Abazajian, P. Agrawal, Z. Chacko and C. Kilic, JCAP **11** (2010), 041 doi:10.1088/1475-7516/2010/11/041 [arXiv:1002.3820 [astro-ph.HE]].
- [20] K. N. Abazajian and M. Kaplinghat, Phys. Rev. D **86** (2012), 083511 doi:10.1103/PhysRevD.86.083511 [arXiv:1207.6047 [astro-ph.HE]].
- [21] K. S. Babu and R. N. Mohapatra, Phys. Rev. D **89** (2014), 115011 doi:10.1103/PhysRevD.89.115011 [arXiv:1404.2220 [hep-ph]].
- [22] A. Biswas, D. Majumdar and P. Roy, JHEP **04** (2015), 065 doi:10.1007/JHEP04(2015)065 [arXiv:1501.02666 [hep-ph]].
- [23] K. P. Modak, JHEP **03** (2015), 064 doi:10.1007/JHEP03(2015)064 [arXiv:1404.3676 [hep-ph]].
- [24] R. Krall, M. Reece and T. Roxlo, JCAP **09** (2014), 007 doi:10.1088/1475-7516/2014/09/007 [arXiv:1403.1240 [hep-ph]].
- [25] J. C. Park, S. C. Park and K. Kong, Phys. Lett. B **733** (2014), 217-220 doi:10.1016/j.physletb.2014.04.037 [arXiv:1403.1536 [hep-ph]].
- [26] M. T. Frandsen, F. Sannino, I. M. Shoemaker and O. Svendsen, JCAP **05** (2014), 033 doi:10.1088/1475-7516/2014/05/033 [arXiv:1403.1570 [hep-ph]].
- [27] S. Baek and H. Okada, [arXiv:1403.1710 [hep-ph]].
- [28] S. Andreas, T. Hambye and M. H. G. Tytgat, JCAP **10** (2008), 034 doi:10.1088/1475-7516/2008/10/034 [arXiv:0808.0255 [hep-ph]].
- [29] W. B. Lu and P. H. Gu, Nucl. Phys. B **924** (2017), 279-311 doi:10.1016/j.nuclphysb.2017.09.005 [arXiv:1611.02106 [hep-ph]].

- [30] M. Kakizaki, A. Santa and O. Seto, Int. J. Mod. Phys. A **32** (2017) no.10, 1750038 doi:10.1142/S0217751X17500385 [arXiv:1609.06555 [hep-ph]].
- [31] W. L. Guo and Y. L. Wu, JHEP **10** (2010), 083 doi:10.1007/JHEP10(2010)083 [arXiv:1006.2518 [hep-ph]].
- [32] A. Merle, Int. J. Mod. Phys. D **22** (2013), 1330020 doi:10.1142/S0218271813300206 [arXiv:1302.2625 [hep-ph]].
- [33] Y. G. Kim, K. Y. Lee and S. Shin, JHEP **05** (2008), 100 doi:10.1088/1126-6708/2008/05/100 [arXiv:0803.2932 [hep-ph]].
- [34] M. Klasen and C. E. Yaguna, JCAP **11** (2013), 039 doi:10.1088/1475-7516/2013/11/039 [arXiv:1309.2777 [hep-ph]].
- [35] T. Hambye and M. H. G. Tytgat, Phys. Lett. B **683** (2010), 39-41 doi:10.1016/j.physletb.2009.11.050 [arXiv:0907.1007 [hep-ph]].
- [36] T. Hambye, JHEP **01** (2009), 028 doi:10.1088/1126-6708/2009/01/028 [arXiv:0811.0172 [hep-ph]].
- [37] S. Bhattacharya, P. Ghosh and N. Sahu, JHEP **02** (2019), 059 doi:10.1007/JHEP02(2019)059 [arXiv:1809.07474 [hep-ph]].
- [38] J. Fiaschi, M. Klasen and S. May, JHEP **05** (2019), 015 doi:10.1007/JHEP05(2019)015 [arXiv:1812.11133 [hep-ph]].
- [39] S. Matsumoto, Y. L. S. Tsai and P. Y. Tseng, JHEP **07** (2019), 050 doi:10.1007/JHEP07(2019)050 [arXiv:1811.03292 [hep-ph]].
- [40] S. Batebi, M. Haghighat, S. Tizchang and H. Akafzade, Int. J. Mod. Phys. A **30** (2015) no.20, 1550108 doi:10.1142/S0217751X15501080 [arXiv:1410.7725 [hep-ph]].
- [41] M. M. Ettefaghi, Phys. Rev. D **79** (2009), 065022 doi:10.1103/PhysRevD.79.065022 [arXiv:0903.1708 [hep-ph]].
- [42] M. Hayakawa, Phys. Lett. B **478** (2000), 394-400 doi:10.1016/S0370-2693(00)00242-2 [arXiv:hep-th/9912094 [hep-th]].
- [43] M. Hayakawa, [arXiv:hep-th/9912167 [hep-th]].
- [44] X. Calmet, B. Jurco, P. Schupp, J. Wess and M. Wohlgenannt, Eur. Phys. J. C **23** (2002), 363-376 doi:10.1007/s100520100873 [arXiv:hep-ph/0111115 [hep-ph]].
- [45] M. Chaichian, P. Presnajder, M. M. Sheikh-Jabbari and A. Tureanu, Eur. Phys. J. C **29** (2003), 413-432 doi:10.1140/epjc/s2003-01204-7 [arXiv:hep-th/0107055 [hep-th]].

- [46] B. Melic, K. Passek-Kumericki, J. Trampetic, P. Schupp and M. Wohlgenannt, Eur. Phys. J. C **42** (2005), 483-497 doi:10.1140/epjc/s2005-02318-6 [arXiv:hep-ph/0502249 [hep-ph]].
- [47] B. Melic, K. Passek-Kumericki, J. Trampetic, P. Schupp and M. Wohlgenannt, Eur. Phys. J. C **42** (2005), 499-504 doi:10.1140/epjc/s2005-02301-3 [arXiv:hep-ph/0503064 [hep-ph]].
- [48] P. Aschieri, B. Jurco, P. Schupp and J. Wess, Nucl. Phys. B **651** (2003), 45-70 doi:10.1016/S0550-3213(02)00937-9 [arXiv:hep-th/0205214 [hep-th]].
- [49] W. Behr, N. G. Deshpande, G. Duplancic, P. Schupp, J. Trampetic and J. Wess, Eur. Phys. J. C **29** (2003), 441-446 doi:10.1140/epjc/s2003-01207-4 [arXiv:hep-ph/0202121 [hep-ph]].
- [50] J. Gomis and T. Mehen, Nucl. Phys. B **591** (2000), 265-276 doi:10.1016/S0550-3213(00)00525-3 [arXiv:hep-th/0005129 [hep-th]].
- [51] V. Silveira and A. Zee, Phys. Lett. B **161** (1985), 136-140 doi:10.1016/0370-2693(85)90624-0
- [52] J. McDonald, Phys. Rev. D **50** (1994), 3637-3649 doi:10.1103/PhysRevD.50.3637 [arXiv:hep-ph/0702143 [hep-ph]].
- [53] C. P. Burgess, M. Pospelov and T. ter Veldhuis, Nucl. Phys. B **619** (2001), 709-728 doi:10.1016/S0550-3213(01)00513-2 [arXiv:hep-ph/0011335 [hep-ph]].
- [54] C. E. Yaguna, JCAP **03** (2009), 003 doi:10.1088/1475-7516/2009/03/003 [arXiv:0810.4267 [hep-ph]].
- [55] X. G. He, T. Li, X. Q. Li, J. Tandean and H. C. Tsai, Phys. Lett. B **688** (2010), 332-336 doi:10.1016/j.physletb.2010.04.026 [arXiv:0912.4722 [hep-ph]].
- [56] G. Duplancic, P. Schupp and J. Trampetic, Eur. Phys. J. C **32** (2003), 141-144 doi:10.1140/epjc/s2003-01372-4 [arXiv:hep-ph/0309138 [hep-ph]].
- [57] M. M. Ettefaghi, Phys. Rev. D **86** (2012), 085038 doi:10.1103/PhysRevD.86.085038 [arXiv:1210.0500 [hep-ph]].
- [58] F. Calore, I. Cholis, C. McCabe and C. Weniger, Phys. Rev. D **91** (2015) no.6, 063003 doi:10.1103/PhysRevD.91.063003 [arXiv:1411.4647 [hep-ph]].
- [59] A. Albert *et al.* [Fermi-LAT and DES], Astrophys. J. **834** (2017) no.2, 110 doi:10.3847/1538-4357/834/2/110 [arXiv:1611.03184 [astro-ph.HE]].
- [60] M. Ackermann *et al.* [Fermi-LAT], Astrophys. J. **840** (2017) no.1, 43 doi:10.3847/1538-4357/aa6cab [arXiv:1704.03910 [astro-ph.HE]].
- [61] A. Abramowski *et al.* [H.E.S.S.], Phys. Rev. Lett. **106** (2011), 161301 doi:10.1103/PhysRevLett.106.161301 [arXiv:1103.3266 [astro-ph.HE]].

- [62] J. Coronado-Blazquez, M. A. Sanchez-Conde, A. Dominguez, A. Aguirre-Santaella, M. Di Mauro, N. Mirabal, D. Nieto and E. Charles, *JCAP* **07** (2019), 020 doi:10.1088/1475-7516/2019/07/020 [arXiv:1906.11896 [astro-ph.HE]].
- [63] M. Cirelli, G. Corcella, A. Hektor, G. Hutsi, M. Kadastik, P. Panci, M. Raidal, F. Sala and A. Strumia, *JCAP* **03** (2011), 051 doi:10.1088/1475-7516/2012/10/E01 [arXiv:1012.4515 [hep-ph]].
- [64] J. Bovy and S. Tremaine, *Astrophys. J.* **756** (2012), 89 doi:10.1088/0004-637X/756/1/89 [arXiv:1205.4033 [astro-ph.GA]].
- [65] J. F. Navarro, C. S. Frenk and S. D. M. White, *Astrophys. J.* **490** (1997), 493-508 doi:10.1086/304888 [arXiv:astro-ph/9611107 [astro-ph]].
- [66] A. Klypin, H. Zhao and R. S. Somerville, *Astrophys. J.* **573** (2002), 597-613 doi:10.1086/340656 [arXiv:astro-ph/0110390 [astro-ph]].
- [67] F. Calore, I. Cholis and C. Weniger, *JCAP* **03** (2015), 038 doi:10.1088/1475-7516/2015/03/038 [arXiv:1409.0042 [astro-ph.CO]].
- [68] K. N. Abazajian, N. Canac, S. Horiuchi and M. Kaplinghat, *Phys. Rev. D* **90** (2014) no.2, 023526 doi:10.1103/PhysRevD.90.023526 [arXiv:1402.4090 [astro-ph.HE]].
- [69] T. Sjostrand, S. Mrenna and P. Z. Skands, *JHEP* **05** (2006), 026 doi:10.1088/1126-6708/2006/05/026 [arXiv:hep-ph/0603175 [hep-ph]].
- [70] A. W. Graham, D. Merritt, B. Moore, J. Diemand and B. Terzic, *Astron. J.* **132** (2006), 2685-2700 doi:10.1086/508988 [arXiv:astro-ph/0509417 [astro-ph]].
- [71] K. A. Oman, J. F. Navarro, A. Fattahi, C. S. Frenk, T. Sawala, S. D. M. White, R. Bower, R. A. Crain, M. Furlong, M. Schaller, J. Schaye and T. Theuns, *Mon. Not. Roy. Astron. Soc.* **452** (2015) no.4, 3650-3665 doi:10.1093/mnras/stv1504 [arXiv:1504.01437 [astro-ph.GA]].
- [72] J. M. Cline, K. Kainulainen, P. Scott and C. Weniger, *Phys. Rev. D* **88** (2013), 055025 doi:10.1103/PhysRevD.88.055025 [arXiv:1306.4710 [hep-ph]].